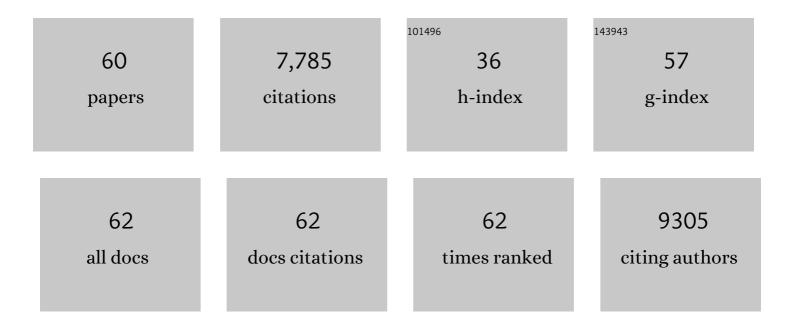
## Albertus Denny Handoko

List of Publications by Year in descending order

Source: https://exaly.com/author-pdf/4864927/publications.pdf Version: 2024-02-01



#	Article	IF	CITATIONS
1	Feasibility of CO2 Capture and Utilization: From the LCA Perspective. , 2022, , 39-53.		0
2	Polaron Delocalization Dependence of the Conductivity and the Seebeck Coefficient in Doped Conjugated Polymers. Journal of Physical Chemistry B, 2022, 126, 2073-2085.	1.2	5
3	High-performance & thermally stable n-type polymer thermoelectrics based on a benzyl viologen radical cation-doped ladder-type conjugated polymer. Journal of Materials Chemistry A, 2021, 9, 11787-11793.	5.2	22
4	Electron n-doping of a highly electron-deficient chlorinated benzodifurandione-based oligophenylene vinylene polymer using benzyl viologen radical cations. Materials Chemistry Frontiers, 2021, 5, 6182-6191.	3.2	4
5	Recent Progress in Extending the Cycleâ€Life of Secondary Znâ€Air Batteries. ChemNanoMat, 2021, 7, 354-367.	1.5	37
6	Selectivity Map for the Late Stages of CO and CO <sub>2</sub> Reduction to C <sub>2</sub> Species on Copper Electrodes. Angewandte Chemie - International Edition, 2021, 60, 10784-10790.	7.2	30
7	Selectivity Map for the Late Stages of CO and CO 2 Reduction to C 2 Species on Copper Electrodes. Angewandte Chemie, 2021, 133, 10879-10885.	1.6	3
8	Thermoelectric Performances of n-Doped Ladder-Type Conjugated Polymers Using Various Viologen Radical Cations. ACS Applied Polymer Materials, 2021, 3, 5596-5603.	2.0	7
9	Sulfurized Cyclopentadienyl Nanocomposites for Shuttle-Free Room-Temperature Sodium–Sulfur Batteries. Nano Letters, 2021, 21, 10538-10546.	4.5	11
10	A High-Performance Magnesium Triflate-based Electrolyte for Rechargeable Magnesium Batteries. Cell Reports Physical Science, 2020, 1, 100265.	2.8	48
11	2H-MoS <sub>2</sub> on Mo <sub>2</sub> CT <sub><i>x</i></sub> MXene Nanohybrid for Efficient and Durable Electrocatalytic Hydrogen Evolution. ACS Nano, 2020, 14, 16140-16155.	7.3	180
12	Rational Design of Two-Dimensional Transition Metal Carbide/Nitride (MXene) Hybrids and Nanocomposites for Catalytic Energy Storage and Conversion. ACS Nano, 2020, 14, 10834-10864.	7.3	349
13	Probing the electronic and geometric structures of photoactive electrodeposited Cu2O films by X-ray absorption spectroscopy. Journal of Catalysis, 2020, 389, 483-491.	3.1	8
14	Defectâ€Enhanced CO <sub>2</sub> Reduction Catalytic Performance in Oâ€Terminated MXenes. ChemSusChem, 2020, 13, 5690-5698.	3.6	59
15	Two-Dimensional Titanium and Molybdenum Carbide MXenes as Electrocatalysts for CO2 Reduction. IScience, 2020, 23, 101181.	1.9	123
16	LCA of electrochemical reduction of CO2 to ethylene. Journal of CO2 Utilization, 2020, 41, 101229.	3.3	38
17	Outstanding Reviewers for <i>Materials Horizons</i> in 2019. Materials Horizons, 2020, 7, 1207-1207.	6.4	0
18	Self-gating in semiconductor electrocatalysis. Nature Materials, 2019, 18, 1098-1104.	13.3	167

#	Article	IF	CITATIONS
19	Catalytic Effect on CO <sub>2</sub> Electroreduction by Hydroxyl-Terminated Two-Dimensional MXenes. ACS Applied Materials & Interfaces, 2019, 11, 36571-36579.	4.0	94
20	Surface-engineered cobalt oxide nanowires as multifunctional electrocatalysts for efficient Zn-Air batteries-driven overall water splitting. Energy Storage Materials, 2019, 23, 1-7.	9.5	48
21	Theory-guided materials design: two-dimensional MXenes in electro- and photocatalysis. Nanoscale Horizons, 2019, 4, 809-827.	4.1	218
22	Ultrathin two-dimensional materials for photo- and electrocatalytic hydrogen evolution. Materials Today, 2018, 21, 749-770.	8.3	228
23	Transitionâ€Metalâ€Doped αâ€MnO <sub>2</sub> Nanorods as Bifunctional Catalysts for Efficient Oxygen Reduction and Evolution Reactions. ChemistrySelect, 2018, 3, 2613-2622.	0.7	54
24	One-Step Facile Synthesis of Cobalt Phosphides for Hydrogen Evolution Reaction Catalysts in Acidic and Alkaline Medium. ACS Applied Materials & Interfaces, 2018, 10, 15673-15680.	4.0	76
25	High-throughput theoretical optimization of the hydrogen evolution reaction on MXenes by transition metal modification. Journal of Materials Chemistry A, 2018, 6, 4271-4278.	5.2	198
26	Tuning the Basal Plane Functionalization of Two-Dimensional Metal Carbides (MXenes) To Control Hydrogen Evolution Activity. ACS Applied Energy Materials, 2018, 1, 173-180.	2.5	304
27	Rational Design of Sulfurâ€Doped Copper Catalysts for the Selective Electroreduction of Carbon Dioxide to Formate. ChemSusChem, 2018, 11, 320-326.	3.6	102
28	Crystal structure and surface characteristics of Sr-doped GdBaCo <sub>2</sub> O <sub>6â^î^</sub> double perovskites: oxygen evolution reaction and conductivity. Journal of Materials Chemistry A, 2018, 6, 5335-5345.	5.2	42
29	Elucidation of thermally induced internal porosity in zinc oxide nanorods. Nano Research, 2018, 11, 2412-2423.	5.8	10
30	Understanding heterogeneous electrocatalytic carbon dioxide reduction through operando techniques. Nature Catalysis, 2018, 1, 922-934.	16.1	515
31	Establishing new scaling relations on two-dimensional MXenes for CO <sub>2</sub> electroreduction. Journal of Materials Chemistry A, 2018, 6, 21885-21890.	5.2	138
32	On the Role of Sulfur for the Selective Electrochemical Reduction of CO <sub>2</sub> to Formate on CuS <sub><i>x</i></sub> Catalysts. ACS Applied Materials & Interfaces, 2018, 10, 28572-28581.	4.0	157
33	Electrochemical Reduction of CO <sub>2</sub> Using Copper Single-Crystal Surfaces: Effects of CO* Coverage on the Selective Formation of Ethylene. ACS Catalysis, 2017, 7, 1749-1756.	5.5	507
34	–CH <sub>3</sub> Mediated Pathway for the Electroreduction of CO <sub>2</sub> to Ethane and Ethanol on Thick Oxide-Derived Copper Catalysts at Low Overpotentials. ACS Energy Letters, 2017, 2, 2103-2109.	8.8	117
35	Mechanistic Insights into the Selective Electroreduction of Carbon Dioxide to Ethylene on Cu <sub>2</sub> O-Derived Copper Catalysts. Journal of Physical Chemistry C, 2016, 120, 20058-20067.	1.5	164
36	<i>In Situ</i> Raman Spectroscopy of Copper and Copper Oxide Surfaces during Electrochemical Oxygen Evolution Reaction: Identification of Cu <sup>III</sup> Oxides as Catalytically Active Species. ACS Catalysis, 2016, 6, 2473-2481.	5.5	592

#	Article	IF	CITATIONS
37	Mechanistic Insights into the Enhanced Activity and Stability of Agglomerated Cu Nanocrystals for the Electrochemical Reduction of Carbon Dioxide to <i>n</i> Propanol. Journal of Physical Chemistry Letters, 2016, 7, 20-24.	2.1	211
38	Enhanced activity of H2O2-treated copper(ii) oxide nanostructures for the electrochemical evolution of oxygen. Catalysis Science and Technology, 2016, 6, 269-274.	2.1	48
39	Selective Electrochemical Reduction of Carbon Dioxide to Ethylene and Ethanol on Copper(I) Oxide Catalysts. ACS Catalysis, 2015, 5, 2814-2821.	5.5	741
40	Stable and selective electrochemical reduction of carbon dioxide to ethylene on copper mesocrystals. Catalysis Science and Technology, 2015, 5, 161-168.	2.1	292
41	Highly Efficient Photocatalytic H <sub>2</sub> Evolution from Water using Visible Light and Structureâ€Controlled Graphitic Carbon Nitride. Angewandte Chemie - International Edition, 2014, 53, 9240-9245.	7.2	1,000
42	Interfacial charge separation in Cu <sub>2</sub> O/RuO <sub>x</sub> as a visible light driven CO <sub>2</sub> reduction catalyst. Physical Chemistry Chemical Physics, 2014, 16, 5922-5926.	1.3	55
43	Enhanced photoelectrochemical water splitting by nanostructured BiVO4–TiO2 composite electrodes. Journal of Materials Chemistry A, 2014, 2, 3948.	5.2	164
44	Photocatalytic reduction of CO <sub>2</sub> and protons using water as an electron donor over potassium tantalate nanoflakes. Nanoscale, 2014, 6, 9767.	2.8	83
45	Controllable proton and CO2 photoreduction over Cu2O with various morphologies. International Journal of Hydrogen Energy, 2013, 38, 13017-13022.	3.8	121
46	Hydrothermal growth of piezoelectrically active lead-free (Na,K)NbO <sub>3</sub> –LiTaO <sub>3</sub> thin films. CrystEngComm, 2013, 15, 672-678.	1.3	21
47	Recent progress in artificial photosynthesis: CO2 photoreduction to valuable chemicals in a heterogeneous system. Current Opinion in Chemical Engineering, 2013, 2, 200-206.	3.8	95
48	Dimensionally and compositionally controlled growth of calcium phosphate nanowires for bone tissue regeneration. Journal of Materials Chemistry B, 2013, 1, 6170.	2.9	24
49	Hydrothermal epitaxy of lead free (Na,K)NbO3-based piezoelectric films. Materials Research Society Symposia Proceedings, 2013, 1547, 45-52.	0.1	0
50	Piezoelectrically active hydrothermal KNbO3 thin films. CrystEngComm, 2012, 14, 421-427.	1.3	16
51	Understanding the defect structure of solution grown zinc oxide. Journal of Solid State Chemistry, 2012, 189, 63-67.	1.4	9
52	Hydrothermal epitaxy of BiFeO3 films on SrTiO3 substrates. Progress in Crystal Growth and Characterization of Materials, 2011, 57, 109-116.	1.8	5
53	Hydrothermal synthesis of epitaxial NaxK(1â~'x)NbO3 solid solution films. Thin Solid Films, 2011, 519, 5156-5160.	0.8	16
54	Low temperature formation of (NaxK1â^'x)NbO3 from hydrothermally synthesised NaNbO3. Materials Research Innovations, 2011, 15, 352-356.	1.0	8

#	Article	IF	CITATIONS
55	STRESS ANALYSIS OF (001) PREFERRED ORIENTED BiFeO <sub>3</sub> AND Bi(Cr <sub>0.03</sub> Fe <sub>0.97</sub> )O <sub>3</sub> FILMS. Integrated Ferroelectrics, 2010, 113, 9-25.	0.3	1
56	Hydrothermal synthesis of (00l) epitaxial BiFeO3 films on SrTiO3 substrate. CrystEngComm, 2010, 12, 3806.	1.3	25
57	Hydrothermal synthesis of sodium potassium niobate solid solutions at 200 °C. Green Chemistry, 2010, 12, 680.	4.6	46
58	One-Dimensional Perovskite Nanostructures. Science of Advanced Materials, 2010, 2, 16-34.	0.1	20
59	Hydrothermal synthesis of (K,Na)NbO3. Acta Crystallographica Section A: Foundations and Advances, 2008, 64, C594-C594.	0.3	0
60	Time resolved emission spectroscopy investigations of pulsed laser ablated plasmas of ZrO2and Al2O3. Journal of Physics: Conference Series, 2006, 28, 100-104.	0.3	3